Chinese Chemical Letters 35 (2024) 108622

Contents lists available at ScienceDirect

Chinese Chemical Letters

journal homepage: www.elsevier.com/locate/cclet

Dual-additives enable stable electrode-electrolyte interfaces for long life Li-SPAN batteries

Zhenqiang Guo[a,b,1], Huicong Yang[a,b,1], Qian Wei[a,b], Shengjun Xu[a,b], Guangjian Hu[a,b,e,*], Shuo Bai[a,b], Feng Li[a,b,c,d,*]

[a] School of Materials Science and Engineering, University of Science and Technology of China, Shenyang 110016, China
[b] Shenyang National Laboratory for Materials Science, Institute of Metal Research, Chinese Academy of Sciences, Shenyang 110016, China
[c] Department of Biochemistry and Molecular Biology, College of Life Science, China Medical University, Shenyang 110122, China
[d] Dalian National Laboratory for Clean Energy, Dalian 116023, China
[e] Shenyang King Power Technology Co., Ltd., Shenyang 110016, China

ARTICLE INFO

Article history:
Received 27 April 2023
Revised 16 May 2023
Accepted 29 May 2023
Available online 30 May 2023

Keywords:
Sulfurized polyacrylonitrile
Lithium metal
Interface film
2-Fluoropyridine
Difluorobis (oxalato) phosphate

ABSTRACT

Sulfurized polyacrylonitrile (SPAN) is proposed as a promising cathode material for lithium sulfur batteries. However, the continuous side reactions at the electrolyte-electrode interfaces as well as the slow redox kinetics of SPAN cathode deteriorate the electrochemical performance. In this study, an electrolyte with dual-additives comprising 2-fluoropyridine (2-FP) and lithium difluorobis (oxalato) phosphate (LiDFBOP) was used to improve the performance of Li||SPAN cells. 2-FP has a lower lowest occupied molecular orbital energy than that of the solvents in the electrolyte, leading to its prior reduction. A LiF-rich film can be formed on the electrode, effectively improving the stability of the electrolyte-electrode interfaces and prolonging the life. Simultaneously, LiDFBOP could form an electrolyte-electrode interface film containing a large amount of $Li_xPO_yF_z$ species, compensating for the kinetic deterioration caused by the lower ionic conductive of LiF formed at the electrolyte-electrode interface. Hence, an electrode-interface film with good chemical stability and high Li^+ transport was established by LiF and $Li_xPO_yF_z$-rich species. The Li||SPAN cell with the electrolyte containing dual-additives demonstrates an excellent capacity retention of 97.5% after 200 cycles at 1.0 C, 25 °C, comparing to 56.2% capacity retention without additives. Moreover, the rate capacities of cells with dual-additives can reach 1128.1 mAh/g at 5 C, comparing to only 813.5 mAh/g using electrolyte without additives. Our results shown that the dual-additives in electrolyte provide a promising strategy for practical application of lithium sulfur batteries with SPAN cathodes.

Lithium-ion batteries have revolutionized the market for electric vehicles, energy storage and portable electronic devices with many advantages, such as low self-discharge rate and high energy density [1]. However, to further meet the electrification trend of society, lithium-based batteries with higher energy density and lower cost [2,3] are urgently needed. Lithium-sulfur (Li-S) batteries, owing to the high theoretical energy density and low cost for the abundant sulfur resources on the earth [4,5], is one of the most promising lithium-based batteries for application. However, the formation of soluble lithium polysulfide (LiPS) species, which can deteriorate cycling performance, reduce capacity utilization, and corrode the lithium metal anode, is a key factor hindering the application of Li-S batteries [6]. In recent years, various strategies have been proposed to solve these LiPS shuttling problems by cathode design [7,8]. Among them, sulfur-containing polymer instead of monomeric sulfur as the cathode, especially sulfurized polyacrylonitrile (SPAN), has shown the advantages and is promising for high performance Li-S batteries [9,10]. This is because that the SPAN can completely eradicate the shuttle of LiPSs because of the absence of polysulfide [11]. However, the slow redox reaction kinetics of short-chain sulfur, the fragile cathode-electrolyte interface (CEI) film, and the unstable anode-electrolyte interface (SEI) film of the SPAN cathode hinder the application of Li||SPAN cells [12,13].

Electrolyte regulation is one of the main approaches to address the above problems in Li||SPAN cells. The equal volume mixture of ethylene carbonate (EC) and diethyl carbonate (DEC) with 1.0 mol/L lithium hexafluorophosphate ($LiPF_6$) is the most common electrolyte system in Li||SPAN cells. However, its practical application in Li||SPANcells is limited by rapid capacity decay and

* Corresponding authors at: School of Materials Science and Engineering, University of Science and Technology of China, Shenyang 110016, China.
E-mail addresses: gjhu@imr.ac.cn (G. Hu), fli@imr.ac.cn (F. Li).
[1] These authors contributed equally to this work.

https://doi.org/10.1016/j.cclet.2023.108622
1001-8417/

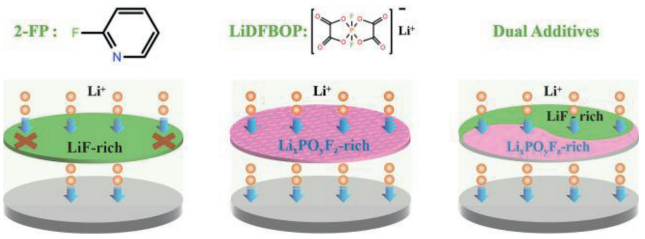

Scheme 1. The combined effect mechanism of dual-additives in the formation of electrode-electrolyte interface.

short lifespan [14,15]. The main drawback of carbonate electrolyte is the unstable SEI film formed at the lithium metal anode and electrolyte interface for the poor reduction stability of EC and DEC solvents [16]. And this can lead to the formation of lithium dendrites [17] and dead lithium [18] during Li^+ plating/stripping, thus greatly reduce the Coulombic efficiency of the lithium metal anode [19]. In addition to the lithium metal anode, the continuous side reactions between the SPAN cathode and EC would also deteriorate the electrochemical performance of Li||SPAN cells [20]. Therefore, building a more stable electrode-electrolyte interface is the key to face these challenges. And the functional additives reasonably in the electrolyte is the effective and most economical method [21].

Owing to its electrically insulating properties, high mechanical strength and chemical stability, LiF is considered a good component to stabilize SEI and CEI films and effectively reduce the side reactions between electrolyte and electrode [22] for enhancing the performance of Li||SPAN cells. In recent years, many fluorinated organic additives, like fluoroethylene carbonate (FEC) [23], trimethylsilyl(fluorosulfonyl)(*n*-nonfluorobutanesulfonyl)imide (TMS-FNFSI) [24], tris(2,2,2-trifluoroethyl)borate (TTFEB) [25] and (trifluoroethoxy)pentafluorocyclotophosphazene (TFPN) [26], *etc*., have been reported to form LiF-rich electrode-electrolyte interfaces. Besides the additives mentioned above, fluoropyridine, as a new class of fluorinated organic additives, has recently received much attention due to its effective solubility of lithium salt, wide electrochemical window and excellent SEI film forming ability [27–29]. After gaining electrons, fluoropyridine is easily reduced to form LiF-rich SEI films on the lithium metal anode surface, thus guiding the uniform nucleation of lithium ions [30]. However, despite the many positive effects of LiF, the transportation ability of Li^+ in the LiF-rich electrode interface film is limited by the low ionic conductivity of LiF ($\approx 10^{-12}$ S/cm) [31]. Therefore, in order to simultaneously enhance the kinetics of the redox reaction in Li||SPAN cells, it is also necessary to improve the Li^+ transport. It was found that when lithium salts were used as film-formation additives, the resulting interface films from additives are more ionically conductive because lithium ions are incorporated into the electrode interface films [32]. Recently, a phosphorus-based lithium salt additive, lithium difluorobis (oxalato) phosphate (LiDFBOP), can be reduced to form an interface film on the anode surface before the solvent, and the phosphorus derivatives from LiDFBOP facilitate rapid Li^+ transport, resulting in a low interfacial impedance [33]. Therefore, it is a promising strategy to use 2-fluoropyridine (2-FP) and lithium LiDFBOP together as additives in EC-based electrolyte to solve the problems of poor cycling stability and slow redox reaction kinetics of Li||SPAN cells by constructing electrode interface films with good chemical stability and high Li^+ transport.

Here, an EC-based electrolyte with dual-additives (0.5 wt% 2-FP and 0.5 wt% LiDFBOP) for Li||SPAN cells is proposed. As shown in Scheme 1, benefiting from the combined effect of 2-FP and LiDFBOP, LiF and $Li_xPO_yF_z$-rich species can be formed on both anode and cathode surfaces to build electrode-electrolyte interfaces with good chemical/electrochemical stability and high Li^+ transport. The Li||SPAN cell with dual-additives demonstrates an excellent capacity retention of 97.5% after 200 cycles at 1.0 C as well as a good rate performance of 1128.1 mAh/g at 5 C.

Ethylene carbonate (EC), diethyl carbonate (DEC), lithium hexafluorophosphate ($LiPF_6$), lithium perchlorate ($LiClO_4$) and lithium difluorobis(oxalato) phosphate (LiDFBOP) were purchased from DodoChem and used as received. 2-Fluoropyridine (2-FP) was obtained from Aladdin. For electrolyte preparation, $LiPF_6$ or $LiClO_4$ was directly dissolved in EC and DEC (1:1 by weight ratio) mixed solvents. And the concentration of lithium salt in electrolyte is 1 mol/L. Electrolytes containing 0.5 wt%, 1.0 wt% and 2.0 wt% 2-FP, 0.25 wt%, 0.5 wt%, 1.0 wt% and 2.0 wt% LiDFBOP and dual-additives (0.3-0.7 wt% 2-FP and 0.3-0.7 wt% LiDFBOP) were prepared by blending adequate amounts of salts and solvents in glass bottle, and further stirred for one night at room temperature. All the experimental work above was carried out in an Ar-filled glove box (<0.1 ppm water, <1.0 ppm O_2) as well as the materials storage used in this study.

Sulfur powder (S) and polyacrylonitrile (PAN) were obtained from Aladdin and were mixed by ball-milling at a mass ratio of 2:1. The mixture was then heat-treated at 350 °C for 6 h in argon atmosphere and finally cooled to room temperature to obtain SPAN [34]. The sulfur content in obtained SPAN is 37% measured by element analysis.

For fabricating the cathode, 70 wt% SPAN powder, 10 wt% binder (PVDF) and 20 wt% Super P were mixed in the *N*-methylpyrrolidone (NMP) solvent and uniformly coated on the carbon-coated aluminum foil. The obtained SPAN cathodes were dried at 60 °C for one night in a vacuum oven to remove the solvent and moisture then cut to disks with a diameter of 12 mm. 2025-coin cells were assembled using the above-prepared SPAN cathode, lithium metal anode of 16 mm diameter and 200 μm thick, and electrolyte. A microporous membrane polypropylene film (Celgard 2400) with a thickness of 25 μm was used as a separator. The sulfur loading of SPAN electrodes was about 1 mg/cm^2, and the electrolyte used in the study was 40 μL/mg$_{sulfur}$. Li||Cu cells were assembled with Li foil and Cu foil as electrodes. Li||Li symmetric cells were assembled with Li metal as both cathode and anode. All coin cells were assembled in an argon-filled glove box.

Li||SPAN pouch cells were fabricated using Celgard 2400 separator sheets sandwiched between the SPAN electrode (size: 8.7 by 8.8 cm) and the 50 μm Li metal anode. All pouch cells were assembled in a drying room and electrolyte injection was performed in an argon-filled glove box, and 1 ml electrolyte was injected into each cell.

The Li||SPAN cells were charged and discharged at a constant current in the voltage range of 1.0-3.0 V by a LAND 2001 A battery system, the loading of active substance is the actual content of sulfur. Li||SPAN cells were activated at 0.1 C (1 C = 1675 mAh/g) for three cycles before cycling, and then the cycling test was performed at 1 C. Cyclic voltammetry (CV) measurements and electrochemical impedance spectroscopy (EIS) were conducted using a Bio-Logic VSP-300 electrochemical workstation. The CV of Li||SPAN cells and Li||Cu cells were measured at the scan rate of 0.2 mV/s and 1.0 mV/s, respectively. The EIS of Li||SPAN cells were measured in the frequency range from 100 kHz to 15 mHz. The morphology of the cycled electrode was observed by scanning electron microscopy (SEM, Verios G4 UC) and transmission electron microscope (TEM, Tecnai F20). The component differences of the electrode surface were studied by X-ray photoelectron spectroscopy (XPS, ES-CALAB 250 with Al Ka radiation, 1486.6 V, 150 W) under 4×10^{-8} Pa. To investigate the components in formed SEI layers, the Cu electrodes after lithium electro-stripping/deposition cycling were analyzed by time-of-flight secondary ion mass spectrome-

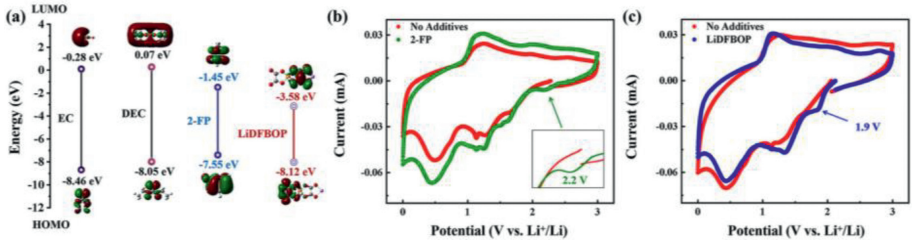

Fig. 1. (a) The LUMO and HOMO energies of EC, DEC, 2-FP and LiDFBOP. (b) The CV curves of Li||Cu cells using the electrolyte with and without 2-FP. (c) The CV curves of Li||Cu cells using the electrolyte with and without LiDFBOP.

try (TOF-SIMS) using a mass spectrometer (TOF SIMS-5, ION-TOF) equipped with a 30 keV Bi^+ primary ion gun.

The highest occupied molecular orbital (HOMO) and the lower lowest occupied molecular orbital (LUMO) energy of solvents (EC and DEC) and additive molecules (2-FP and LiDFBOP) were calculated by the Gaussian 16 program package. The B3LYP functional with a basis set of 6–311+G(d, p) was employed to optimize the structures of the molecules.

First, to determine the reduction ability of additives, the LUMO and HOMO energies of LiDFBOP and 2-FP were calculated in comparison with EC and DEC solvents. As shown in Fig. 1a, the LUMO energies of EC, DEC, 2-FP and LiDFBOP are -0.28, 0.07, -1.45 and -3.58 eV, respectively. Both 2-FP and LiDFBOP exhibit significantly lower LUMO energies than those of EC and DEC, indicating the preferential reduction of 2-FP and LiDFBOP on the anode to form SEI [27,33]. To further confirm the results of theoretical calculations, CV tests of Li||Cu cells were adopted to measure the exact reduction potentials of two additives. As shown in Fig. 1b, the electrolyte with 2-FP shows a reduction peak at 2.2 V, which is due to the decomposition of 2-FP on Cu surface. For the electrolyte with LiDFBOP, there is a clear reduction peak at 1.9 V (Fig. 1c) [33]. The reduction potentials of both additives are in the operating voltage range of Li||SPAN batteries, indicating that 2-FP and LiDFBOP can be reduced on both anode-electrolyte and cathode-electrolyte interfaces.

To determine the optimal additive content, the effects of different single additive contents on the electrochemical impedance of Li||SPAN cells were analyzed. Fig. S1 (Supporting information) presents the impedance of Li||SPAN cells with different contents of 2-FP (0.5, 1.0 and 2.0 wt%). The impedance increases significantly with 2-FP content, which was attributed to the large amount of LiF generated on the interface film by the excess organic 2-FP additive. Fig. S2 (Supporting information) is the impedance of Li||SPAN cells in electrolytes with different contents of LiDFBOP (0.25, 0.5, 1.0 and 2.0 wt%). At LiDFBOP additions of 0.25 wt% and 0.5 wt%, the impedance was lower than that of the cell without additives, and the impedance was lowest at 0.5 wt%. However, the opposite results were presented at higher LiDFBOP contents (1.0 and 2.0 wt%), which may be related to the large amount of additives leading to side reactions.

According to the above analysis, it can be reasonably inferred that the optimal amounts of dual-additives (2-FP and LiDFBOP) should be no more than 1 wt%. Furthermore, a cycle test was presented to confirm the effect of different mass ratios of 2-FP and LiDFBOP on Li||SPAN cells at a total addition of 1 wt%. Fig. S3 (Supporting information) shows the cycle performance of cells with different mass ratios of 2-FP to LiDFBOP. The cell shows the best cycle performance when the mass ratio of 2-FP and LiDFBOP is 0.5 wt%:0.5 wt%. Hence, it can be reasonably inferred that the 0.5 wt% 2-FP and 0.5 wt% LiDFBOP is an optimal ratio, which is used as dual-additives for the following experiments.

Since both 2-FP and LiDFBOP have a lower LOMO level than EC and DEC, they can be easier reduced on the anode surface, which can be helpful for forming a stable anode-electrolyte interface. To confirm this, the effect of additives on the reversibility of Li plating and stripping was investigated by Li||Cu cells (Fig. 2a). As shown in Fig. 2d, the CE values of Li||Cu with the electrolyte without additives, with 2-FP, with LiDFBOP and with dual-additives are 85.1%, 88.0%, 88.8% and 92.3%, respectively. The lower CE of the electrolyte without additives implies the greater loss of active lithium, and the poor reductive stability of electrolyte against lithium [35]. When 2-FP and/or LiDFBOP were added, the CE increased obviously, indicating both 2-FP and LiDFBOP can effectively improve the reversibility of lithium metal anode, and increase the compatibility of lithium metal with EC-based electrolyte. The voltage profiles of Li||Cu cells with different additives are displayed in Figs. 2a and b. The nucleation and plateau overpotentials in the electrolyte with LiDFBOP were significantly lower than those without LiDFBOP, confirming that LiDFBOP can effectively improve the kinetics, especially alleviating the kinetics deterioration caused by 2-FP.

Li||Li symmetric cells at 1.0 mA/cm^2 (1.0 mAh/cm^2) was conducted to further investigate the stability of the lithium metal anode in the electrolyte without and with different additives. As shown in Fig. 2c, the electrolyte without additives displayed a sharply increased over-potential after 365 h. For the electrolyte with LiDFBOP, the overpotential is much smaller than the electrolyte without additives, indicating that LiDFBOP can improve the kinetics, but the lifespan is only slightly increased. The electrolyte with 2-FP has a significantly longer cycle life and remains more stable after the 900 h, but have a larger voltage polarization in the early stages of the cycle. For the electrolyte with dual additives, the cells exhibited the smallest voltage hysteresis and the longest cycle life of over 1300 h, which was much better than the cells without additives and with single additive. Therefore, the above experimental results have confirmed that the combined effect of dual-additives can significantly prolong the cycling life of lithium metal anode.

The EIS results of the Li||Li cells after 20 cycles are shown in Fig. 2e. The lower impedance of the cells without additives may be related to the large specific surface area of the lithium dendrites generated by the unstable SEI film. However, the addition of 2-FP resulted in a significant increase in impedance, although it significantly improved the cycling stability, which is consistent with the charge-discharge polarization of Li||Cu cells. When 2-FP and LiDFBOP were used together, a suitable impedance is obtained. The morphological changes of electrodeposition can also verify the function of dual-additives, as Figs. 2f and g showing the deposited Li on the anode surface after 200 cycles. A loose Li deposition layer with obvious needle-like lithium dendrites were formed on the lithium metal anode of the electrolyte without additives, causing the continuous electrolyte consumption and deteriorating the performance. For the electrolyte with LiDFBOP, although no obvious needle-like Li dendrites were observed, lots of loose and cracked structure could be observed on the surface of lithium metal anode (Fig. S4 in Supporting information). After introduction of 2-FP, a large number of porous structures could still be observed on

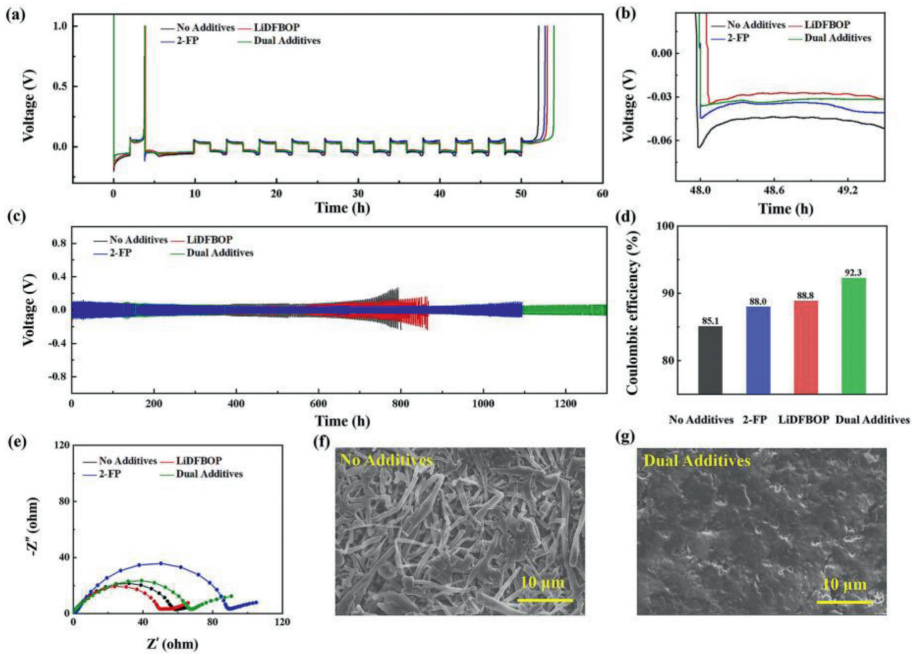

Fig. 2. (a) Voltage profiles of Li||Cu cells. (b) The amplification of voltage profiles in (a). (c) Voltage profiles of Li||Li symmetric cells. (d) The average CE of the electrolyte without and with additives. (e) The EIS curves of the Li||Li cell using electrolyte without and with additives after 20 cycles. (f, g) The morphologies of the deposited Li on the anode surface after 200 cycles.

the surface of lithium metal anode. In comparison, with the dual-additive, the surface of lithium metal anode remains dense and uniform after cycling, presenting a dendrite-free morphology. The above experimental results confirmed that the dual-additives can significantly improve the electrochemical performance of lithium metal anode, which is attributed to the stable and fast ionic conductive SEI layer obtained by the combined effect of 2-FP and LiDFBOP.

XPS was performed to further investigate the mechanism of electrolyte additives in the formation of SEI film. Since LiF is one of the main products in SEI film, $LiClO_4$ was used instead of $LiPF_6$ to exclude interference of $LiPF_6$ to determine that LiF comes from the decomposition of the additive but not from the lithium salt. For the electrolyte with 2-FP, the products containing F and N element were detected on the SEI film (Fig. S5 in Supporting information). In the F containing products, the peaks located at 684.6 eV and 687.1 eV correspond to LiF and C-F, respectively. In the N containing products, the peak located at 399.1 eV is corresponding to Li_3N while that located at 400.5 eV is related to pyridine N [30]. For the electrolyte with LiDFBOP, in the F 1s spectra, the peak appears at 684.9 eV, 687.3 eV and 688.8 eV, corresponding to LiF, P-F($Li_xPO_yF_z$) and C-F, respectively (Fig. S6 in Supporting information) [32]. In the P 2p spectra, a relatively stronger $Li_xPO_yF_z$ peak (135.9 eV) and a weaker P-F peak (138.9 eV) are also observed [33]. Since only the additive contains the elements F, P or N, these products can only originate from the reduction reaction of additives. TOF-SIMS measurements were performed to further characterize the SEI components. As shown in Figs. S7 and S8 (Supporting information), for the electrolyte with 2-FP, the species with F^-, $CH_2CH_2N^-$, and $C_4H_4F^-$ were detected in the negative mode at $m/z = 19$, 42 and 71, respectively. And the species with Li_3N^+, LiF and $C_5H_9N^+$ were detected in the positive mode at $m/z = 32$, 33 and 83, respectively. For the electrolyte with LiDFBOP, the species with F^-, PO_2^- and PO_3^- appear in the negative mode at $m/z = 19$, 63 and 79 [36], respectively. And $m/z = 33$ and $m/z = 123$ correspond to LiF and $LiPO_3F_2$ species in the positive mode, respectively. Therefore, for the electrolyte with 2-FP, its main reaction products on the SEI film include LiF, Li_3N, $C_5H_9N^+$. For the electrolyte with LiDFBOP, the main decomposition products are LiF and $LiPO_3F_2$.

For better understanding the combined effect of 2-FP and LiDFBOP on the formation of SEI film, XPS was also conducted on the cycled lithium metal anode. Fig. 3 shows the XPS spectra results of lithium metal anode in the electrolyte with and without additives. According to the F 1s spectra, in the electrolyte with LiDFBOP, the content of LiF slightly increases, suggesting that the decomposition of LiDFBOP produces a small amount of LiF. The peak intensity of LiF of the electrolyte with 2-FP is significantly enhanced than that without 2-FP. A LiF-rich SEI film can effectively improve the mechanical stability and compactness of lithium metal anode [37]. Meanwhile, LiF has insulation characteristics, which can effectively reduce the penetration of electrons through the anode interface, which can prevent the side reaction between electrolyte and electrode, and improve the cycle stability [38]. For the dual-additives, a significantly stronger LiF peak can also be observed, which is mainly attributed to the reduction of two additives. In the P 2p spectra, the electrolyte with LiDFBOP has much stronger peak for $Li_xPO_yF_z$, which has been considered as an effective component for Li ion transport capacity of SEI film [33]. Similarly, for the electrolyte with dual-additives, a significantly stronger $Li_xPO_yF_z$ peak was detected. Moreover, the N 1s spectra of anode interface film is displayed in Fig. 3c, the components of pyridine N peak and Li_3N peak could be observed by 2-FP, which can inhibit the formation of lithium dendrites [27]. In contrast, no N 1s spectra was detected in the electrolyte without 2-FP. In general, benefiting from the co-reduction of 2-FP and LiDFBOP, a SEI film rich in LiF, $Li_xPO_yF_z$ and Li_3N can be formed on the anode-electrolyte interface.

In addition to being reduced at the anode side, the reduction species of 2-FP and LiDFBOP can be observed during the discharge process at the SPAN cathode surface according to the CV results shown in Figs. 1b and c. Since LiF is the main product in CEI film, $LiClO_4$ was used instead of $LiPF_6$ to exclude interference of $LiPF_6$. XPS was used to analyze the decomposition products of additives on the SPAN cathode surface during the first discharge. For the electrolyte with 2-FP, the C-F products ($\approx$ 688.0 eV) and LiF ($\approx$ 685.0 eV) were detected during the discharge, as shown in the F 1s

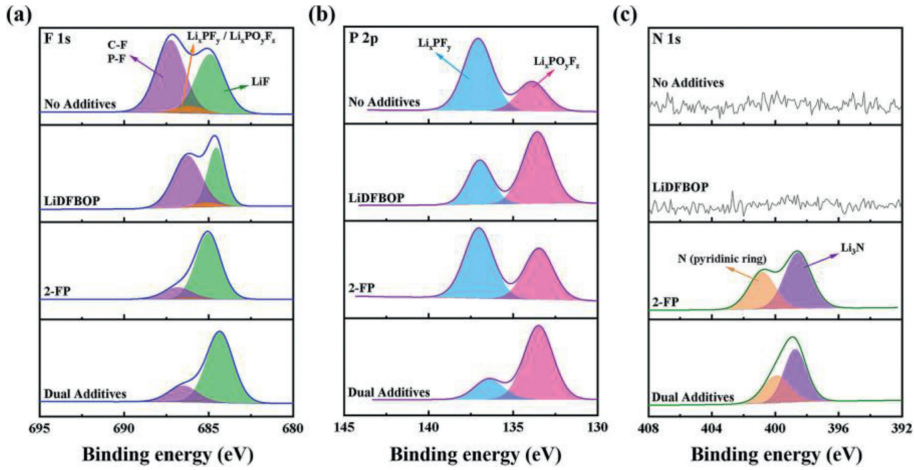

Fig. 3. The XPS spectra results of lithium metal anode after 10 cycles: (a) F 1s, (b) P 2p, (c) N 1s.

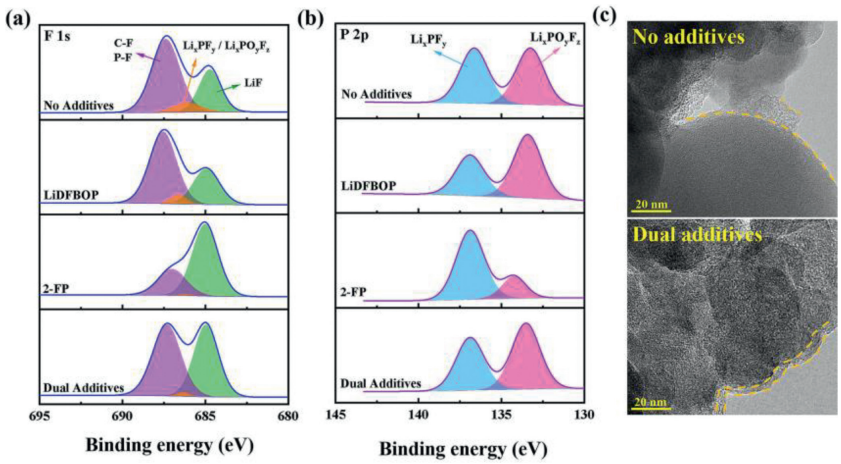

Fig. 4. The XPS spectra results of SPAN electrodes after 200 cycles: (a) F 1s, (b) P 2p. (c) TEM of SPAN-cathode surface morphology after 200 cycles in Li||SPAN cells without and with dual-additives, where the dotted area is the CEI film.

spectra (Fig. S9 in Supporting information). The relative intensity of LiF peak gradually increases during the discharge, which proves that 2-FP can be reduced at the SPAN cathode. For the electrolyte with LiDFBOP, the P-F products (≈ 687.8 eV) and LiF (≈ 684.7 eV) were detected in the F 1s spectra (Fig. S10 in Supporting information). The relative intensity of LiF peak gradually increases during the first discharge. In the P 2p spectra (Fig. S11 in Supporting information), $Li_xPO_yF_z$, one of the main reduction products of LiDFBOP, shows a consistent trend with LiF. The above results demonstrate that LiDFBOP can also be reduced at the SPAN cathode.

To investigate the CEI film formation mechanism of dual-additives, XPS analysis was performed on the cycled SPAN (Figs. 4a and b). For the electrolyte with LiDFBOP, a rich $Li_xPO_yF_z$ species were detected on the cycled cathode, and a small amount of Li_xPF_y indicates that the suppressed decomposition of electrolyte. For the electrolyte with 2-FP, a LiF-rich CEI film was formed. LiF can play an active role in stabilizing the CEI film to reduce the side reactions between the cathode and the electrolyte [39]. For electrolytes with dual additives, a large number of LiF and $Li_xPO_yF_z$ species were detected on the cathode surface. It is due to the combined effect of these two additives that the dual-additives provide a significant performance advantage over electrolytes without additives or with a single additive.

SEM was used to observe the morphology of electrode surface after 200 cycles of Li||SPAN cells to confirm the formation of stable CEI, as displayed in Fig. S12 (Supporting information). In the electrolyte without additives, the surface of the SPAN reveals coarse and porous, which aggravates the consumption of electrolyte. As to the SPAN cycled with LiDFBOP, porous structures are also observed. In comparison, for the electrolyte with 2-FP and dual additives, the cycled cathode exhibits a smoother and regular interface morphology. Furthermore, the TEM images of the cycled SPAN were also analyzed for further demonstrate the difference in CEI film (Fig. 4c). An uneven thick and irregular CEI film can be observed on the cycled SPAN surface using the electrolyte without additives and even some areas are not covered with CEI film (as shown in the dotted area), which is recognized to contribute to the capacity decay. For the electrolyte with dual-additives, the cathode is covered by a thin and complete amorphous film, proving that the CEI formed by dual-additives may play a vital role in protecting the cathode.

The performances of additives toward Li||SPAN cells were evaluated by electrochemical measurements. Firstly, to get a clear understanding of the internal redox reactions, CV curves were measured for Li||SPAN cells with and without additives as shown in Fig. 5a. There are two reduction peaks at 1.97 V and 1.69 V of Li||SPAN cells without additives, corresponding to the transformation from short chain sulfur to Li_2S. The oxidation peak is located at 2.37 V is attributed to the rebuilding of short chain-like sulfur [40], and the redox potential difference is 0.68 V. After adding 2-FP to the electrolyte, a large oxidation peak appears at 2.41 V, a small reduction peak appears at 1.60 V. The redox potential dif-

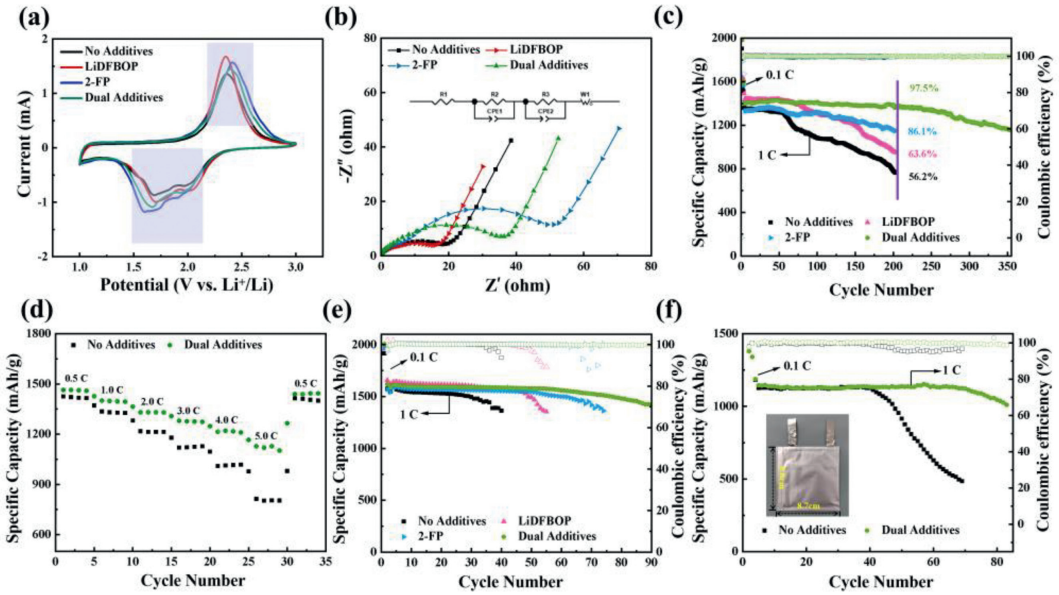

Fig. 5. (a) CV curves of Li||SPAN cells in the electrolyte with or without additives after activation. (b) EIS curves of Li||SPAN cells with the electrolyte with or without additives after activation. (c) Cycle performance of Li||SPAN cells in the electrolyte without additives, with LiDFBOP, with 2-FP, and with dual-additives. (d) Rate performance. (e) Cycle performance of Li||SPAN cells at 60 °C in the electrolyte without additives, with LiDFBOP, with 2-FP, and with dual-additives. (f) Cycle performance of Li||SPAN pouch cells at 25 °C in the electrolyte with dual-additives and without additives.

ference is increased by 0.13 V. However, for the electrolyte with LiDFBOP, a small oxidation peak and a reduction peak can be observed at 2.35 V, 1.71 V, respectively, the redox potential difference is decreased by 0.04 V, proving that LiDFBOP can improve the cell kinetics [33]. For the electrolyte with dual additives, the oxidation peak appears at 2.40 V, the lowest reduction peak appears at 1.67 V, the redox potential difference is 0.73 V, implying that LiDFBOP can effectively reduce the slow kinetics caused by 2-FP. Fig. 5b shows the EIS curve of Li||SPAN cells. The semicircle in the high-frequency region corresponds to the impedance (R_{sei}) of lithium ions passing through the passivation film on the electrode surface, and the intermediate frequency region is the impedance of charge transfer (R_{ct}) [41]. 2-FP significantly increases the impedance of the cell ($R_{cell} = R_{sei} + R_{cei} + R_{ct}$) (Table S1 in Supporting information), while LiDFBOP can effectively decreases the impedance, which agrees well with the results of the CV measurement.

The long-term performance of Li||SPAN cells with and without additives were tested (Fig. 5c). The electrolyte without additives showed a rapidly capacity fading. Only a specific capacity of 764.3 mAh/g is left after 200 cycles with a capacity retention of 56.2%. By comparison, the specific capacity of the cells with 2-FP, LiDFBOP, and dual-additives electrolytes are 1145.8, 948.8 and 1363.7 mAh/g with capacity retentions of 86.1%, 63.6% and 97.5%, respectively. These significant differences prove the advantages of dual-additives in improving the cycling stability of Li||SPAN cells. In addition, the electrolyte with dual-additives in this work also has excellent cell performance comparing to most related literature (Table S2 in Supporting information) [34,42–49]. Furthermore, the charge-discharge profiles of the 1st, 100th, 200th and 300th cycles of the electrolyte with and without additives in Fig. S13 (Supporting information) indicate the high electrochemical reversibility of dual-additives. Fig. S14 (Supporting information) shows the EIS curve of the Li||SPAN cell after 200 cycles, and the corresponding fitting results are shown in Table S1. The value of R_{cell} without additives increased from 15.0 Ω to 33.3 Ω, which was due to the electrolyte decomposition during cycling and the continuous formation of unstable electrode interface film. The value of R_{cell} with 2-FP decreased from 51.2 Ω to 29.8 Ω, which reveals that 2-FP can promote the formation of a stable and dense electrode interface film. The value of R_{cell} with LiDFBOP increased slightly from 12.6 Ω to 17.2 Ω, which may be due to the fact that the decomposition products of LiDFBOP at the electrode interface do not protect the electrode well. The value of R_{cell} with dual additives decreased from 36.7 Ω to 22.9 Ω, which indicates that the dual-additives can derive a much more stable and allow fast Li^+ conductive electrode interface film. The above results show that the dual-additives can improve both the cycle stability and kinetics of Li||SPAN cells.

Moreover, the cell using the electrolyte with dual-additives can deliver excellent rate performance. As shown in Fig. 5d, the cell with dual-additives was found to deliver superior discharge capacities of 1464.1, 1400.3, 1330.9, 1280, 1214.6 and 1128.1 mAh/g at 0.5, 1.0, 2.0, 3.0, 4.0 and 5.0 C, respectively, which are all higher than the discharge capacities of 1425.3, 1335.9, 1217.8, 1119.8, 1009.8 and 813.5 mAh/g for the cells without additives. The electrolyte with dual-additives also exhibits a superior charge and discharge voltage platform and a smaller polarization than the electrolyte without additives (Fig. S15 in Supporting information).

To further verify the effect of additives on Li||SPAN cells performance, high temperature (60 °C) cycling performance was also tested. As shown in Fig. 5e, the capacity of the electrolyte without additives dropped drastically after 25 cycles. By comparation, the capacity fast fading phenomenon of the cells with 2-FP and LiDFBOP electrolytes extends to the 48th and 37th cycle, respectively. The electrolyte with dual-additives exhibits high stability for 90 cycles and a CE of about 100%. The improvement of cycling performance can be attributed to the stable and high Li^+ transport interface produced by dual-additives, which effectively inhibits the dissolution and reconstruction of the SEI film at high temperatures and reduces the side reactions between the electrolyte and the electrodes.

Moreover, to show the potential application of the electrolyte with dual-additives, Li||SPAN pouch cells based on the electrolyte with dual-additives were fabricated (Fig. 5f) with an N/P of 3.52, and a capacity of about 40 mAh at 0.1 C. The Li||SPAN pouch cell with dual-additives could deliver a reversible specific capacity of 1137.4 mAh/g after 60 cycles at 25 °C, with a capacity retention of 95.7%. However, the capacity of the pouch cell without additives

drops rapidly after 36 cycles, and only with a capacity retention of 46.6% after 60 cycles, which is similar to that in the literature [12].

In conclusion, a dual-additives electrolyte was proposed to enhance the cycling stability and kinetics of Li||SPAN cells by the combined effect of LiF and $Li_xPO_yF_z$ species. 2-FP can be preferentially reduced on the electrode surface to form a LiF-rich SEI/CEI film, which significantly improve the stability of the electrode. However, Li^+ transport is limited by the low ionic conductivity of LiF. This negative effect can be eliminated by the dual-additives design. LiDFBOP can be decomposed on the electrode surface to generate $Li_xPO_yF_z$ with high ionic conductivity. As a result, the dual-additives electrolyte enabled Li||SPAN cells with excellent cycling capacity retention of 97.5% after 200 cycles at 1 C, in sharp contrast with 56.2% in without additives. Through the combined effect of the above dual-additives, the Li-SPAN battery shows excellent electrochemical performance, which provides strong support for the commercial use of such additives.

Declaration of competing interest

The authors declare that they have no known competing financial interests or personal relationships that could have appeared to influence the work reported in this paper.

Acknowledgments

The authors acknowledge financial support from the National Natural Science Foundation of China (Nos. 52072378, 22209189), the National Key R&D Program of China (No. 2022YFB3803400), the Strategic Priority Research Program of the Chinese Academy of Sciences (Nos. XDA22010602 and 2022YFB3803400) and Shenyang Science and Technology Program (No. 22-322-3-19).

Supplementary materials

Supplementary material associated with this article can be found, in the online version, at doi:10.1016/j.cclet.2023.108622.

References

[1] M. Ryu, Y.K. Hong, S.Y. Lee, J.H. Park, Nat. Commun. 14 (2023) 1316.
[2] J. Kang, D.Y. Han, S. Kim, J. Ryu, S. Park, Adv. Mater. 35 (2023) 2203194.
[3] G.H. Al-Shawesh, J.W. Zhu, W. Zhang, et al., Chin. Chem. Lett. 34 (2023) 108190.
[4] D. Wang, H. Xie, Q. Liu, et al., Angew. Chem. Int. Ed. 62 (2023) e202302767.
[5] A. Benitez, D. Brandell, One Earth 5 (2022) 224–226.
[6] Z. Jin, X. Ma, L. Qiu, et al., Ionics 28 (2022) 1157–1166.
[7] P.L. Feng, W.S. Hou, Z. Bai, et al., Chin. Chem. Lett. 34 (2023) 107427.
[8] X.Y. Li, S. Feng, C.X. Zhao, et al., J. Am. Chem. Soc. 32 (2022) 14638–14646.
[9] C.X. Zhao, W.Z. Chen, Z. Meng, et al., EcoMat 3 (2021) e12066.
[10] B. He, Z.X. Rao, Z.X. Cheng, et al., Adv. Energy Mater. 11 (2021) 2003690.
[11] W.J. Chen, B.Q. Li, C.X. Zhao, et al., Angew. Chem. Int. Ed. 59 (2020) 10732–10745.
[12] Z.Y. Shen, W.D. Zhang, S.L. Mao, et al., ACS Energy Lett. 6 (2021) 2673–2681.
[13] S.M. Sabet, N. Sapkota, S. Chiluwal, et al., ACS Sustain. Chem. Eng. 11 (2023) 2314–2323.
[14] Y. Liu, D. Yang, W. Yan, Q. Huang, Y. Wu, iScience 19 (2019) 316–325.
[15] W.J. Chen, C.X. Zhao, B.Q. Li, et al., Energy Environ. Mater. 3 (2020) 160–165.
[16] A.A. Razzaq, G. Chen, X. Zhao, et al., J. Energy Chem. 61 (2021) 170–178.
[17] H.G. Lee, S.Y. Kim, J.S. Lee, Npj Comput. Mater. 103 (2022) 4723.
[18] A. Aleshin, S. Bravo, K. Redquest, K.N. Wood, ACS Appl. Mater. Interfaces 13 (2021) 2654–2661.
[19] S. Fang, Y. Zhang, X. Liu, Chem. Eng. J. 426 (2021) 131880.
[20] H.J. Yang, A. Naveed, Q.Y. Li, et al., Energy Storage Mater. 15 (2018) 299–307.
[21] Y.K. Liu, C.Z. Zhao, J. Du, et al., Small 19 (2022) 2205315.
[22] Y. Deng, M. Wang, C. Fan, C. Luo, J. Gao, Nano Lett. 21 (2021) 1896–1901.
[23] X.Z. Zheng, G.H. Fang, Y. Pan, et al., J. Power Sources 439 (2019) 227081.
[24] B. Tong, J.W. Wang, Z.J. Liu, et al., J. Power Sources 400 (2018) 225–231.
[25] Y.L. Ma, Z.X. Zhou, C.J. Li, et al., Energy Storage Mater. 11 (2018) 197–204.
[26] Y. Li, Y.L. An, Y. Tian, et al., J. Electrochem. Soc. 166 (2019) A2736–A2740.
[27] Q. Wu, Y. Qan, X. Tang, et al., ACS Appl. Energy Mater. 4 (2021) 10234–10243.
[28] Z.K. Xie, Z.J. Wu, X.W. An, et al., Chem. Eng. J. 393 (2020) 124789.
[29] Z.K. Xie, X.W. An, Z.J. Wu, et al., J. Mater. Sci. Technol. 74 (2021) 119–127.
[30] X.X. Ma, X. Shen, X. Chen, et al., Small Struct. 3 (2022) 2200071.
[31] P. Shi, F. Liu, Y.Z. Feng, et al., Small Struct. 16 (2020) 2001989.
[32] T.X. Yang, H.N. Zeng, W.L. Wang, et al., J. Mater. Chem. A 7 (2019) 8292–8301.
[33] B. Liao, H.Y. Li, M.Q. Xu, et al., Adv. Energy Mater. 8 (2018) 1800802.
[34] H.M. Kim, J.Y. Hwang, D. Aurbach, Y.K. Sun, J. Phys. Chem. Lett. 8 (2017) 5331–5337.
[35] B.D. Adams, J.M. Zheng, X.D. Ren, W. Xu, J.G. Zhang, Adv. Energy Mater. 8 (2017) 1702097.
[36] D.N Zhao, J. Wang, H.L. Lu, et al., J. Power Sources 456 (2020) 228006.
[37] T. Deng, L.S. Cao, X.Z. He, et al., Chem 7 (2021) 3052–3068.
[38] S.K. Merso, T.M. Tekaligne, H.H Weldeyohannes, et al., J. Energy Storage 56 (2022) 105955.
[39] Q.Y. Zhang, J.L. Ma, L. Mei, et al., Matter 5 (2022) 1235–1250.
[40] M. Jiang, K.L. Wang, S. Gao, et al., ChemElectroChem 6 (2018) 1365–1370.
[41] X.Y. Wang, X.Z. Wei, H.F. Dai, J. Energy Storage 21 (2018) 618–631.
[42] L. Wang, X.M. He, J.J. Li, et al., Electrochim. Acta 72 (2012) 114–119.
[43] F. Jin, C.J. Hu, C.H. Liu, et al., J. Electroanal. Chem. 835 (2019) 156–160.
[44] F.J. Lin, J.L. Wang, H. Jia, et al., J. Power Sources 223 (2013) 18–22.
[45] Y. Shuai, Z. Zhang, K. Chen, J. Lou, Y. Wang, Chem. Commun. 55 (2019) 2376–2379.
[46] H. Jia, J. Wang, F. Lin, et al., Chem. Commun. 50 (2014) 7011–7013.
[47] Y. Liu, D. Yang, W. Yan, et al., iScience 19 (2019) 316–325.
[48] Y. Zhang, Y. Zhao, Z. Bakenov, D. Gosselink, P. Chen, J. Solid State Electrochem. 18 (2014) 1111–1116.
[49] J. Wang, F. Lin, H. Jia, et al., Angew. Chem. Int. Ed. 53 (2014) 10099–10104.